

## **Pneumatic Atomization of Laundry Detergent Slurries as affected by Solid Particle Size and Concentration**

J. P. Hecht\* and J. A. Stamper  
Process Technologies, Procter & Gamble  
8256 Union Centre Blvd.  
West Chester, OH 45069 USA

D. K. Giles  
Department of Biological & Agricultural Engineering  
University of California, Davis  
Davis, CA 95616 USA

### **Abstract**

A parametric experimental study of pneumatic atomization of concentrated laundry detergent slurries was performed to better understand particle formation in pilot-scale spray dryers. Nine different slurry formulas were tested. The formula space comprised three different particle-size distributions of added solids each at three different volume fractions (0.095, 0.16, and 0.23). The droplet-size distribution at a fixed position 50 cm from the nozzle on the centerline of the spray was measured at air/liquid mass flow ratios of 0.34, 0.47, and 0.63. Two coaxial pneumatic nozzles were used, where the liquid jet diameter was varied from 3.05 mm to 3.45 mm and the air annulus was held constant with inner and outer diameters of 3.81 and 4.57 mm, respectively. The data indicate that the volume median droplet size decreased with increasing air/liquid mass flow ratio, but only slightly for concentrated slurries at higher air flow rates. The data also show only slight differences between the two nozzle sizes used. The droplet size data at the highest solids loading level showed very little variation with air pressure, liquid-orifice size, or solid particle size. Steady-shear rheology measurements were conducted for the different formulations, but the results did not correlate to the atomization data even though the Ohnesorge number was of order unity. The implication of these observations is that the atomization processes for highly concentrated slurries is controlled by a balance between in-traparticle solid-particle/liquid adhesion forces and the turbulent flow field downstream of the nozzle.

---

\*Corresponding author

## Introduction and Motivation

Dry laundry detergent is frequently made by spray drying a concentrated slurry into a powder. Although spray drying is a conceptually simple and easy-to-control process, the theory that links the slurry feed properties, process design, process operation parameters, and product attributes is largely undeveloped.

An important transformation that occurs in a spray dryer is atomization. Drops that are formed during the atomization process become particles during drying. Other important transformations include coalescence and agglomeration, drying, and expansion due to boiling [1]. All of these affect the quality of the product, such as particle size and density. An effective research program must therefore include separate studies of these transformations, since too many simultaneous processes are occurring inside a dryer to understand the process from drying experiments alone.

A laundry detergent slurry is a viscous, non-Newtonian mixture that contains high loadings of suspended solids. The literature contains relatively few works on atomization of this complex material. Those that are available address the use of pressure-swirl nozzles [2,3].

In this study, pneumatic nozzles (also called two-fluid nozzles) are used. Pneumatic nozzles are typically used for only bench and pilot-scale equipments, due to the high cost of large-scale air compression [4].

Pneumatic nozzles have been studied extensively in the literature. A general schematic of the processes occurring during atomization using a coaxial pneumatic nozzle is shown in Figure 1. The liquid exiting the nozzle is subjected to several processes that dictate the resulting drop-size distribution. First, drops or “lumps” of material are shedded off of the liquid surface. This is known as primary atomization. Beyond this region, secondary atomization processes can occur due to turbulence. Larger drops that are subjected to pressure fluctuations in the turbulent field can be broken into smaller drops. Also, the drops that are formed may collide and coalesce [5,6,7]. More detailed mechanistic descriptions of these processes are located in the literature; excellent reviews of the theory of coaxial pneumatic nozzles are given by Lasheras and Hopfinger [6] and by Varga[7].

There are few papers that address the effects of solid particles on atomization. Son and Kihm [8] studied atomization of coal water slurries with different particle sizes of coal and Mulhem, et al. studied the effects of particle size, loading, and the intrinsic liquid viscosity on atomization of idealized slurries [9].

The objective of this study is to develop an understanding of how the droplet size distribution of realistic laundry detergent slurries is affected by:

- Solid particle size and loading

- Atomization air/liquid ratio
- Nozzle diameter

The results can be used to better control particle formation in pilot-scale spray dryers and to understand the important critical parameters of the process.

## Slurry Batch Preparation and Characteristics

Nine slurry formulas were prepared. These were based on a generic formula for laundry detergent slurries. All of the components of this formula were used in the same proportions for each of the nine mixtures, except for the sodium carbonate. Three different size classifications were used for these particles and each of these were added in three different amounts, as shown in Table 1.

The particle size distributions for each of the solid ingredients and relevant statistics are shown in Figure 2. These particle size distributions were measured using a laser diffraction instrument (Sympatec Rodos). The zeolite particles were very fine ( $\sim 5\mu\text{m}$ ) and so were assumed to be part of the “liquid”. The polyethylene glycol particles have a melting temperature ( $\sim 55^\circ\text{C}$ ) lower than the slurry temperature so they were also treated as part of the liquid. The volume fractions of particles added to the slurries were calculated to be 0.095, 0.16, and 0.23 for the 41%, 35%, and 30% moisture content formulas respectively. The added particles partially dissolved in the slurry due to the presence of water in the formulation.

The three different size classifications of sodium carbonate were prepared in the following manner. The as-received sodium carbonate was screened through a  $250\mu\text{m}$  (60 mesh screen) vibratory screener (Sweco Model No.530S666). These were the “large” particles. The particles that were too large for this screen were milled (Fitz, Homoloid Machine, vaned rotor with a  $0.51\text{mm}$  hole screen) and screened through the same vibratory screener. The particles passing through this screen were the “medium” particles. A second portion of the as-received sodium carbonate was run through a larger mill (Netzsch, 5.5kW) to make the “small” particles. All of the as-received sodium sulfate was screened using the same vibratory screener and the fines were used in the slurry mixtures. Photographs of the sodium carbonate and sodium sulfate particles are shown in Figure 3.

Each slurry batch was prepared in a custom mixer with a low-speed orbital paddle and a high-shear rotating wheel. The preweighed and preheated liquid ( $65^\circ\text{C}$ ) was added to a jacketed pot. The paddle was operated at 30 RPM while the solids were slowly added, starting with the polyethylene glycol and continuing with the zeolite, sodium sulfate, and sodium carbonate. The high shear mixer was then operated for a period of one minute at a speed of 2500 RPM.

The rheology of each slurry was measured with a cup-and-bob rheometer (AR2000, TA Instruments Ltd., 5.920 mm annular gap). The results indicated that the fluid was non-Newtonian. The samples exhibited shear-thinning behavior and yield stresses, so a Herschel-Bulkley model was used to parameterize the data:

$$\mu = \frac{\sigma_y}{\dot{\gamma}} + k \cdot \dot{\gamma}^{n-1} \quad (1)$$

Where  $\mu$  = apparent viscosity, Pa·s

$k$  = consistency, Pa·s<sup>n</sup>

$n$  = shear index

$\sigma_y$  = yield stress, Pa

$\dot{\gamma}$  = shear rate, s<sup>-1</sup>

The results of the measurements are shown in Figure 4 along with the best-fit Herschel-Bulkley model parameters. It should be mentioned though that due to the highly-correlative nature of the Herschel-Bulkley model, our flow curves do not enable us to assign a physical interpretation to the separate parameters. The experimentally-determined apparent viscosity at a shear-rate of 1000s<sup>-1</sup> is also shown in Figure 4 as a comparison between formulations in an atomization-relevant regime.

The slurry density varied from 1.44 to 1.78 kg/l. The temperature of the slurry was 57 ± 4°C.

### Nozzle Characteristics

Two different coaxial pneumatic nozzles were used. Both of these nozzles started as Spraying Systems siphon nozzles (part no. 120150 with a 180 air cap). The outer and inner diameters of the air annulus were 4.57 and 3.81 mm, respectively. The liquid tube diameter in the center of the nozzle was the standard 3.05mm for one nozzle and was machined out to 3.45mm for the second nozzle. Photographs, cross-sections, and diagrams of the nozzles are shown in Figure 5.

The mass flow of air was measured as a function of air pressure by measuring the rate of pressure drop in a tank of a known volume during discharge through the nozzle. The results were within 10% of the values reported by Spraying Systems. The air/liquid mass-flow ratios were 0.34, 0.47, and 0.63 for gauge air pressures of 2.07, 3.10, and 4.14 bar, respectively.

### Experimental Apparatus and Procedure

The overall experimental apparatus is shown in Figure 6. The slurry batch was discharged from the jacketed mixing tank to the nozzle with a piston pump. A thermocouple and pressure transducer recorded the temperature and pressure of the slurry just before atomization. Due to instrumentation failures, the pressure readings were generally unreliable and so are not reported here.

An Oxford Laser System (Oxford Digisize) was used to collect droplet-size-distribution data. This in-

strument acquires high-resolution video images by backlighting the spray with a diffuse laser. The images are then analyzed to yield droplet size distributions. Droplet sizes were measured 50 cm from the nozzle tip on the centerline of the spray.

Personal protective equipment, including chest waders, lab coats, gloves, and personal breathing devices were used due to the caustic nature of the spray.

The flow rate of the slurry in each experiment was 500 ± 25 g/min. The batch size was approximately 15 kg, so each batch lasted approximately 30 minutes. During each batch, the first nozzle was used and data were collected for all three atomizing air pressures before switching to the second nozzle.

At each condition, *i.e.* a nozzle and an air pressure, at least two replicate runs were completed. Each of these replicates usually contained at least 10,000 drops. The data presented in this paper are a combination of the replicates for each condition; in most cases, at least 20,000 drops are represented. In some cases, the first nozzle was tested again as an additional replicate after all of the six conditions for a given batch were run. The experimental results were quite consistent among all of the replicates.

Drops with a measured diameter greater than 350 micrometers were not considered in this analysis since even a single, anomalous drop of this size noticeably shifts the volume-based statistics. A total of four drops were discarded from the entire data set of 1.1 x 10<sup>6</sup> drops, one drop in each of four runs. The statistics were manually recalculated in these cases.

### Results: Qualitative Observations

The sprays all had a very narrow cone angle (~10 degrees), as shown in Figure 7. The cone angle tended to decrease with increasing air pressure as the photos suggest.

Early in the experimentation, before the relevant experimental space was defined, some tests were run at an air/liquid mass ratio of only 0.23 (1.04 bar gauge pressure). The atomization at this air pressure was so visibly poor that we decided not to study this pressure.

Additionally, we originally were intending to try a third nozzle with a liquid core diameter of 2.54mm (Spraying Systems 100150, 180 air cap), but that nozzle repeatedly clogged on the particles in the slurry. The other nozzle sizes never clogged.

## Results: Atomization Data

All of the experimental results are shown in Table 2. These data are then used in a series of nine additional figures for clarity.

### *Effect of Air/Liquid Mass Ratio on Droplet Size*

The volume median diameters as a function of air/liquid mass ratio for slurries containing 9.5, 16, and 23 volume percent solids are shown in Figures 8, 9, and 10. Most of the data indicate that higher air/liquid mass ratios lead to smaller droplets. This effect is always true when comparing air/liquid ratios of 0.34 and 0.47. The volume median droplet size was usually only slightly lower for the highest air/liquid ratio of 0.63. In some cases, *e.g.* for the smaller nozzle, the drop size actually increased at this higher air pressure, although the magnitude of the observed increase was quite small.

A decreasing droplet size is expected for a higher air/liquid mass ratio through a nozzle. This is a well-known trend in the field of liquid atomization [10].

### *Effect of Solid Particle Size on Droplet Size*

The volume median diameters as a function of the volume median diameters of the added solid particles are shown in Figures 11, 12, and 13.

The data in Figure 11 show that for the slurries containing 9.5 volume percent added solids, the droplet size decreased with increasing solid particle size for the larger nozzle and remained either substantially unchanged or larger in the case of the smaller nozzle. In Figure 12, the 16% volume percent added solids, the particle size always decreased for increasing solid particle size from small to medium particle sizes, then usually slightly increased for the largest particles. In Figure 13, the most concentrated slurries, the droplet size remained practically unchanged with the change in solid particle size.

Other researchers have observed a decrease in droplet size with an increase in solid particle size [8,9]. Mulhem, et. al. [8], conducted a force balance on an agglomerate in a turbulent air stream. The tensile strength of the agglomerate was given by the surface forces of the liquid bridges between particles. This force is proportional to the specific surface area of the solid particles and so is inversely proportional to the diameter of the particles for a given solid volume fraction.

The mechanism proposed by Mulhem, et al. is also supported by the qualitative observation that atomization is quite poor at an air/liquid ratio of 0.23, but seems to be nearly independent of air pressure once good atomization is achieved. This implies that there is a “threshold” atomization air pressure that is needed to overcome the strength of the liquid bridges holding the particles together within drops. Atomization data at

more air/liquid mass ratios are necessary to better evaluate this idea.

### *Effect of Solid Particle Loading on Droplet Size*

The volume median diameters as affected by the solids volume fraction for slurries containing small, medium, and large sodium carbonate particles are shown in Figures 14, 15, and 16.

In interpreting these data, it is important to note that although each figure contains three plots of one size of added sodium carbonate, every slurry contained the same sodium sulfate particles, so the overall added particle size also depends on the particle loading. The volume median diameters of the particles added to each slurry are shown on these figures. Since the sodium sulfate particles ( $D_{v,0.5} = 156 \mu\text{m}$ ) were similar in size to the large sodium carbonate particles ( $D_{v,0.5} = 199 \mu\text{m}$ ), the loading level had less of an effect on the solid particle size distribution on the runs shown in Figure 16, than on Figures 14 and 15.

The effect of the volume fraction of solids on the droplet size is therefore illustrated most clearly by Figure 16. The droplet size decreases with increasing solids loadings, but the effect is slight. It is also interesting to note that the nozzle size has very little effect on the results in Figure 16, especially at high air/liquid ratios.

In Figures 14 and 15, the data show that the droplet size is generally lower for slurries containing higher volume fractions of solids. However, these Figures also show that the droplet size is more sensitive to the air/liquid mass ratio for slurries containing a lower volume fraction of solids. The result of this effect is that at higher air/liquid ratios, the droplet size can be larger for higher volume fractions of solids.

### *Effect of Nozzle Size (Liquid Diameter) on Droplet Size*

The nozzle choice does impart some modest differences to the process. The air annulus was the same for both nozzles; the differences are the liquid diameter and the thickness of the “lip” that separates the air from the liquid. The difference in the liquid orifice diameter results in a difference of the liquid velocity as it exits the nozzle. The 13% difference in liquid diameter translates into a 28% difference in liquid velocity since the flow rate was constant. This is really not very significant considering that the liquid velocity was of order 1 m/s and the air velocity was of order 100 m/s.

The data in this paper show that in some cases the volume median diameter is affected by the liquid orifice of the nozzle. These differences can be seen by inspection of Table 2 or any of the Figures 8 to 16. In most cases, the larger diameter nozzle produced larger drops. Figure 14, which contains data for slurries using small sodium carbonate particles, shows this trend consistently. This trend gradually reverses or fades away in

Figures 15 and 16, where medium to large sodium carbonate particles are used.

The reason for the effect of the nozzle size on the droplet size is not straightforward. Given that the differences between the nozzles are geometrically subtle, and the air annulus is the same for both nozzles, the differences probably arise from the primary atomization mechanism as illustrated in Figure 1; one would expect the far flow field to be similar for both nozzles. Extending this argument to the findings in drop-size data suggest that primary atomization is a controlling mechanism for data that are affected by the change of nozzles, whereas atomization results that are not sensitive to this change, such as those for large particles, are more sensitive to secondary atomization processes than primary atomization.

#### *Effect of Rheology on Droplet Size*

In atomization processes, the effect of viscosity is typically evaluated using an Ohnesorge number, which is the ratio of viscous forces to surface tension forces:

$$Oh = \frac{\mu}{(\rho_{liquid} \cdot \sigma \cdot D_1)^{0.5}} \quad (2)$$

Where  $D_1$  = diameter of liquid jet, m

$\mu$  = liquid viscosity, kg/ms

$\rho_{liquid}$  = liquid density, kg/m<sup>3</sup>

$\sigma$  = surface tension, N/m (~0.03 in this case)

Since the viscosity depends on the shear rate, as shown in Figure 4, it is not entirely clear which value to use in Equation 2. However, Oh is typically of order unity when using the viscosity values over the expected shear range. Even though it should be important to the process, the rheology data did not correlate to the atomization results. Perhaps measurements at higher shear rates would be more relevant. Also the rheology data were taken under steady-shear conditions. Thixotropic effects may be very important considering the fast time scale of atomization.

#### **Results: Droplet-size Distributions**

Droplet-size distributions are reported in Figure 17 for the 3.05 mm nozzle for the slurries containing the highest and lowest solids loadings and the highest and lowest sodium carbonate particle size using an air/liquid ratio of 0.63. The distributions clearly show the emergence of a bimodal distribution when the large sodium carbonate particles are used. This larger peak is due to the measurement of the large particles themselves, which will not change by atomization. Mulhem et al [9] also noted this effect and proved the occurrence of the separation of the solid particles from the liquid under high air flow conditions by comparing the volume of the larger mode with the volume of the added particles.

#### **Conclusions**

In Figure 1, several important steps during the atomization process are shown. The fluid mechanics of the atomization process using a coaxial pneumatic nozzle have been studied extensively [6,7], but the problem is still not completely solved. This is particularly true for the viscous, non-Newtonian, and solids-laden fluids in this study. One of the most important mechanisms that contributes to the atomization process is coalescence [5-7]. While coalescence of Newtonian drops has been studied extensively, no studies were found that treat the collision dynamics of drops containing solids.

Despite the lack of a fundamental description of all of the relevant mechanistic processes, several notable conclusions resulted from this study:

1. Droplet size from atomizing slurry through a given nozzle can be controlled with air pressure unless the solids loading is very high. In that case, the droplet size is not very sensitive to this lever.
2. The liquid diameter of the nozzle does not greatly affect atomization. A larger nozzle is less likely to clog; there does not seem to be any advantage to using a smaller nozzle.
3. Slurries containing larger particles at equal volume loadings of solid particles generally form smaller drops.
4. Slurries containing higher volume loadings of particles generally form smaller drops, but at very high solids loadings, this dependence fades.
5. Slurries containing high volume fractions of solids were not very dependent on any of the independent variables in this study (air/liquid mass-flow ratios, solid particle size, nozzle diameter). The far-nozzle flow field is a likely controlling factor for these materials. The size and shape of the air annulus was not varied in this study, but would affect this flow field and should be varied in future studies.
5. Steady-shear rheology data did not correlate to the atomization data in this study.
6. Using high air/liquid ratios in conjunction with slurries containing large volume fractions of large drops is not recommended for spray drying since separation between the solid particles and the slurry liquid can occur during atomization.

#### **References**

1. Huntington, D.H., *Drying Technology*, 22, 6, 1261-1288 (2004)
2. Masters, K., *Spray Drying in Practice*, Gershof Grafisk, Denmark, 169 (2002)
3. Sudlow, C.A, and Mumford, C.J., *Atomization and Sprays*, 4, 6, 629-642 (1994)
4. Pidaparthy, S.R., *Characteristics of Non-Newtonian Detergent Slurry Sprays formed Using Pressure-Swirl Atomizers*, M.S. Thesis, Purdue University (2004)

5. Hecht, J.P., Stamper, J.A., and Giles, D.K., *ILASS Americas, 18<sup>th</sup> Annual Conference on Liquid Atomization and Spraying Systems*, Irvine, CA May 2005.
6. Lasheras, J.C., Hopfinger, E.J., *Annu. Rev. Fluid Mech.*, 32, pg. 275-300 (2000)
7. Varga, C.M., *Atomization of a Small-Diameter Liquid Jet by a High-Speed Gas Stream*, Ph.D. Dissertation, University of California, San Diego (2002)
8. Son, S.Y., and Kihm, K.D., *Atomization and Sprays*, 8, 5, 503-519 (1998)
9. Mulhem, et al. *Atomization and Sprays*, 13, 2&3, 321-343 (2003)
10. Lefebvre, A.H., *Atomization and Sprays*, Taylor & Francis, pg. 239 (1989)

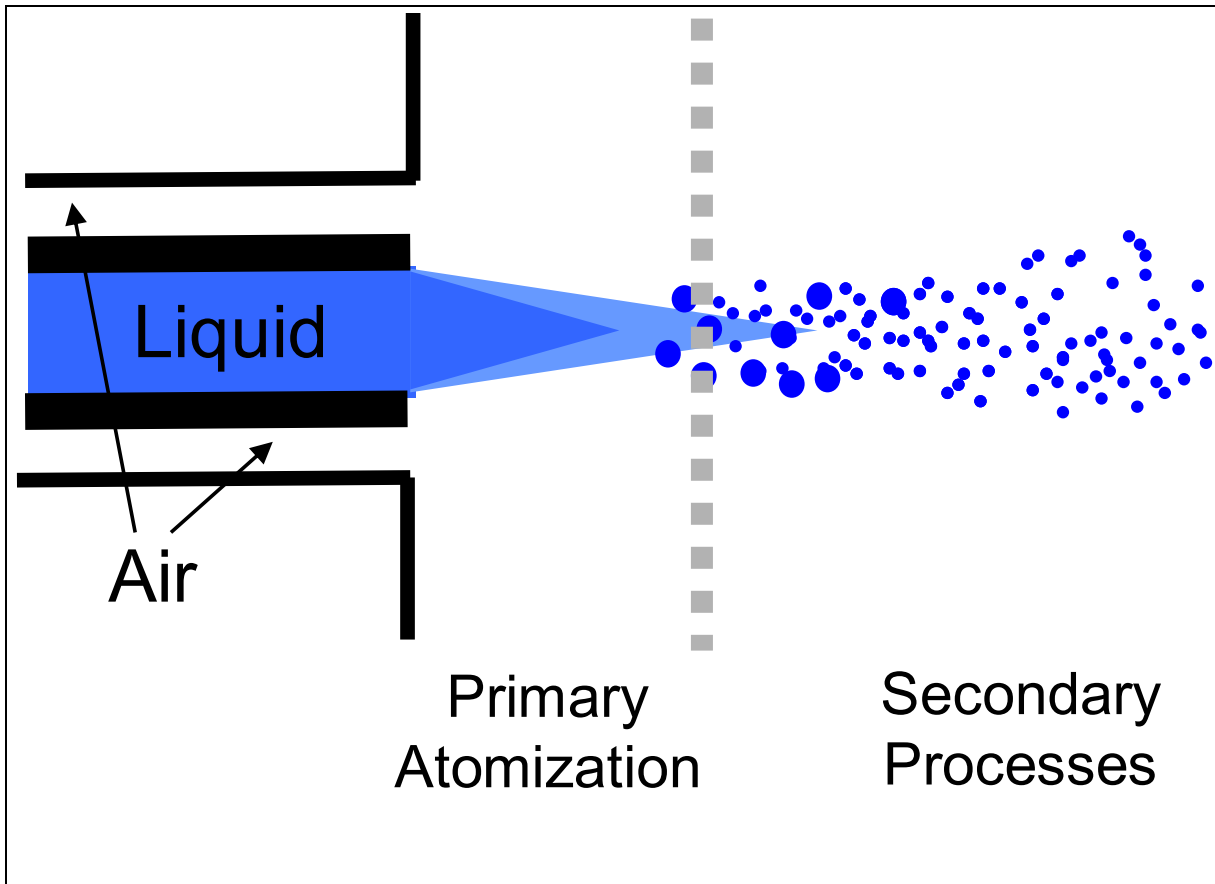


**Figure 1.** Schematic of coaxial atomization processes. Liquid drops and larger masses are shed by the shear of the high-velocity annular air jet. These drops can breakup further due to turbulence. Drops can also coalesce further downstream due to turbulence-induced collisions where spatial concentrations of droplets are high.

Ingredient	Description	Supplier	High Moisture	Medium Moisture	Low Moisture
Water	Tap water	N/A	40.9%	35.0%	30.1%
Sodium Carbonate (anhydrous)	Dense Soda Ash	Ulrich Chemical Inc.	5.0%	18.5%	30.0%
Sodium Linear Alkylbenzene Sulfonate (surfactant)	Calsoft L-50 Slurry (11.8)	Pilot Chemical	13.1%	11.2%	9.6%
Sodium Silicate Solution	1.6 SiO <sub>2</sub> /Na <sub>2</sub> O/Ratio	PQ Corp.	0.4%	0.3%	0.3%
Polyacrylate	Accusol 445N	Rohm and Haas	2.5%	2.2%	1.9%
Polyethylene Glycol	Molecular wt. 4000	BASF	1.5%	1.3%	1.1%
Sodium Sulfate (anhydrous)	Anhydrous	Cooper Natural Resol	15.4%	13.2%	11.4%
DC-1400 Antifoam	Silicone suspension fluid	Dow Corning	0.2%	0.2%	0.2%
Zeolite (Sodium Aluminosilicate)	Valfor 100	PQ Corp.	20.9%	17.9%	15.4%

**Table 1.** Formulations of slurries. Each percentage is expressed as a water-free quantity even though some of the components are received in a diluted form.

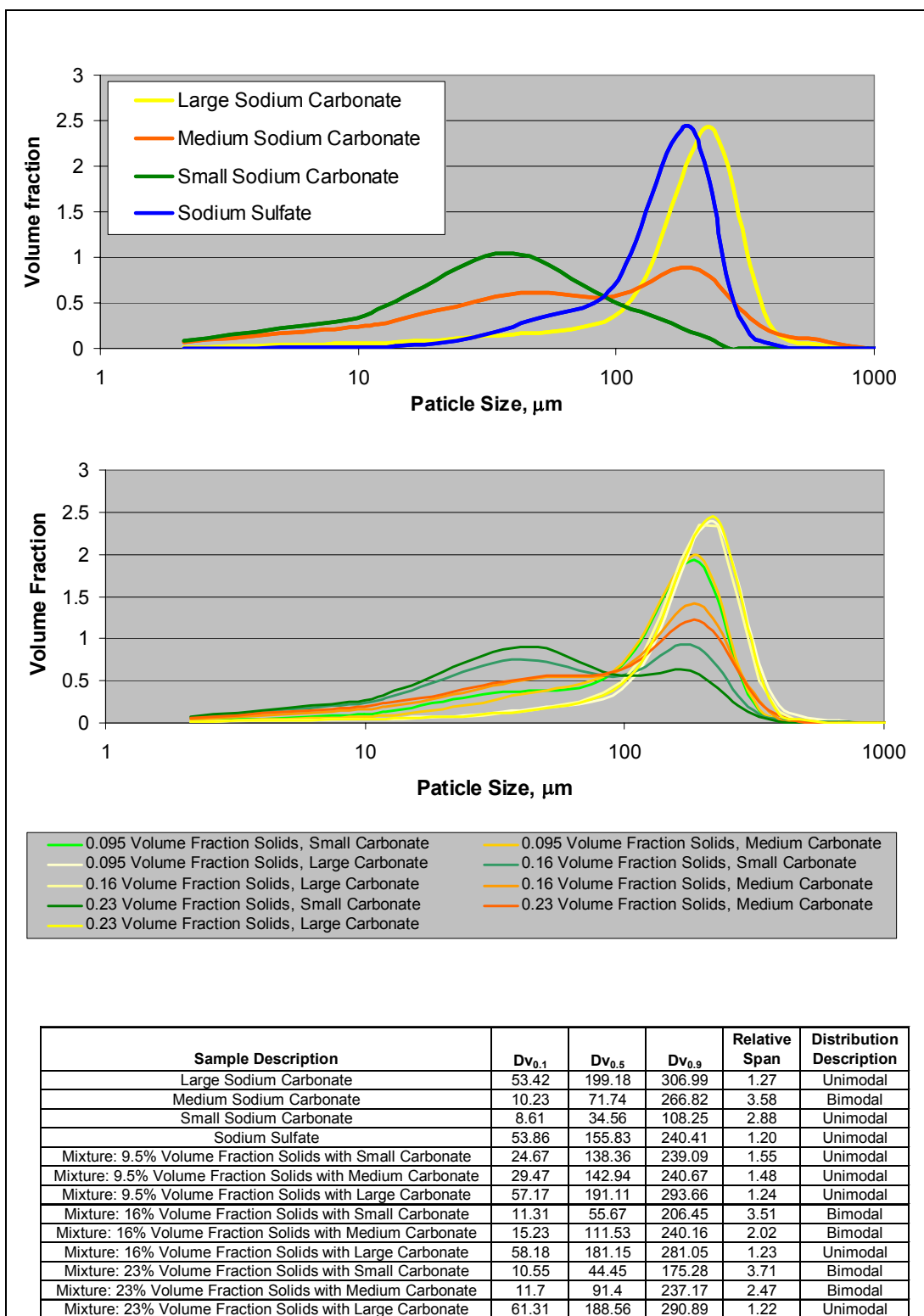
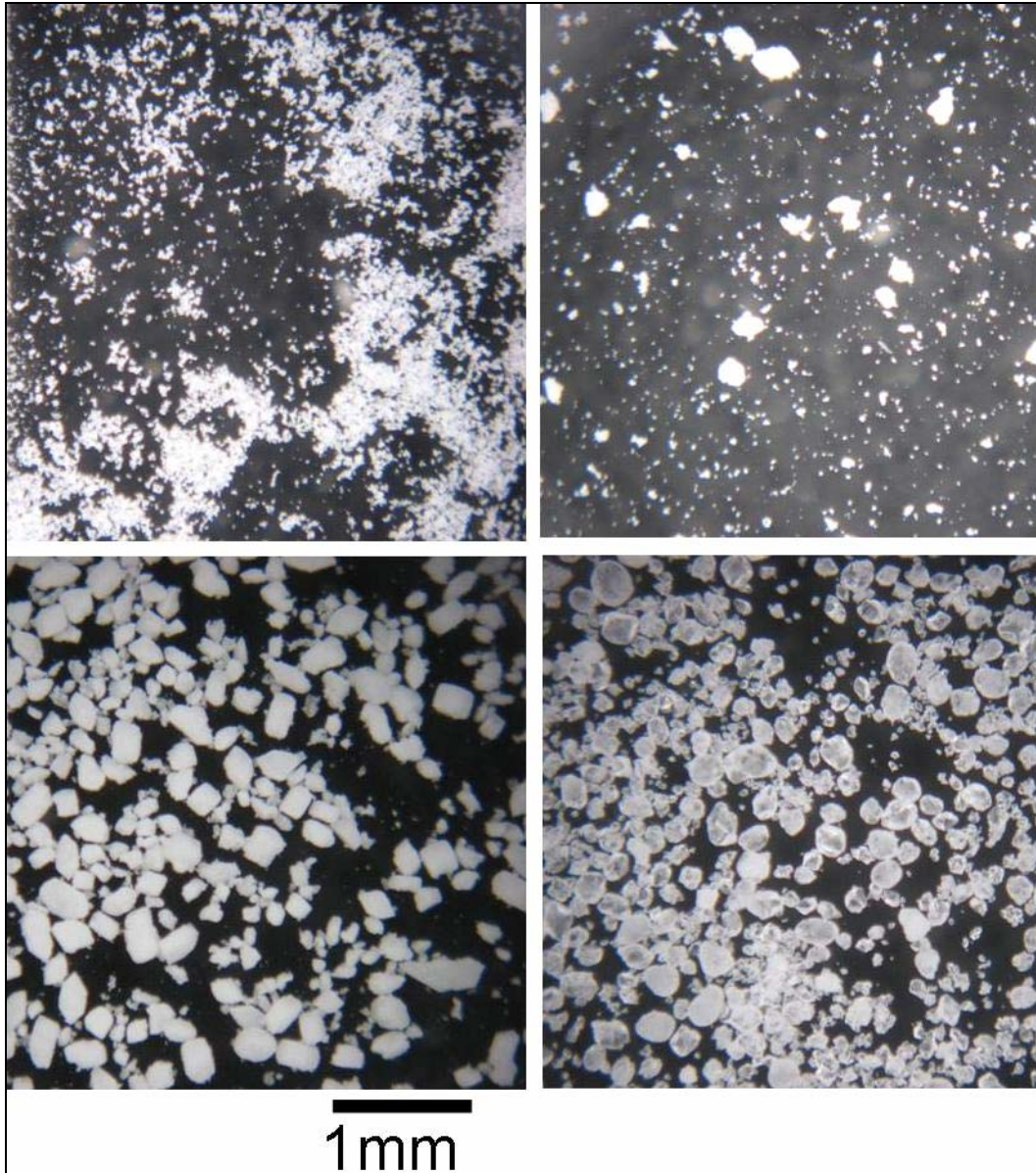


Figure 2. Particle size distributions of sodium carbonate raw materials (top), sodium carbonate/ sodium sulfate mixtures as added to the slurry (middle) and relevant statistics (bottom).



**Figure 3.** Photographs of particles used in slurries. Upper Left: small sodium carbonate. Upper Right: medium sodium carbonate. Lower Left: large sodium carbonate. Lower Right: sodium sulfate

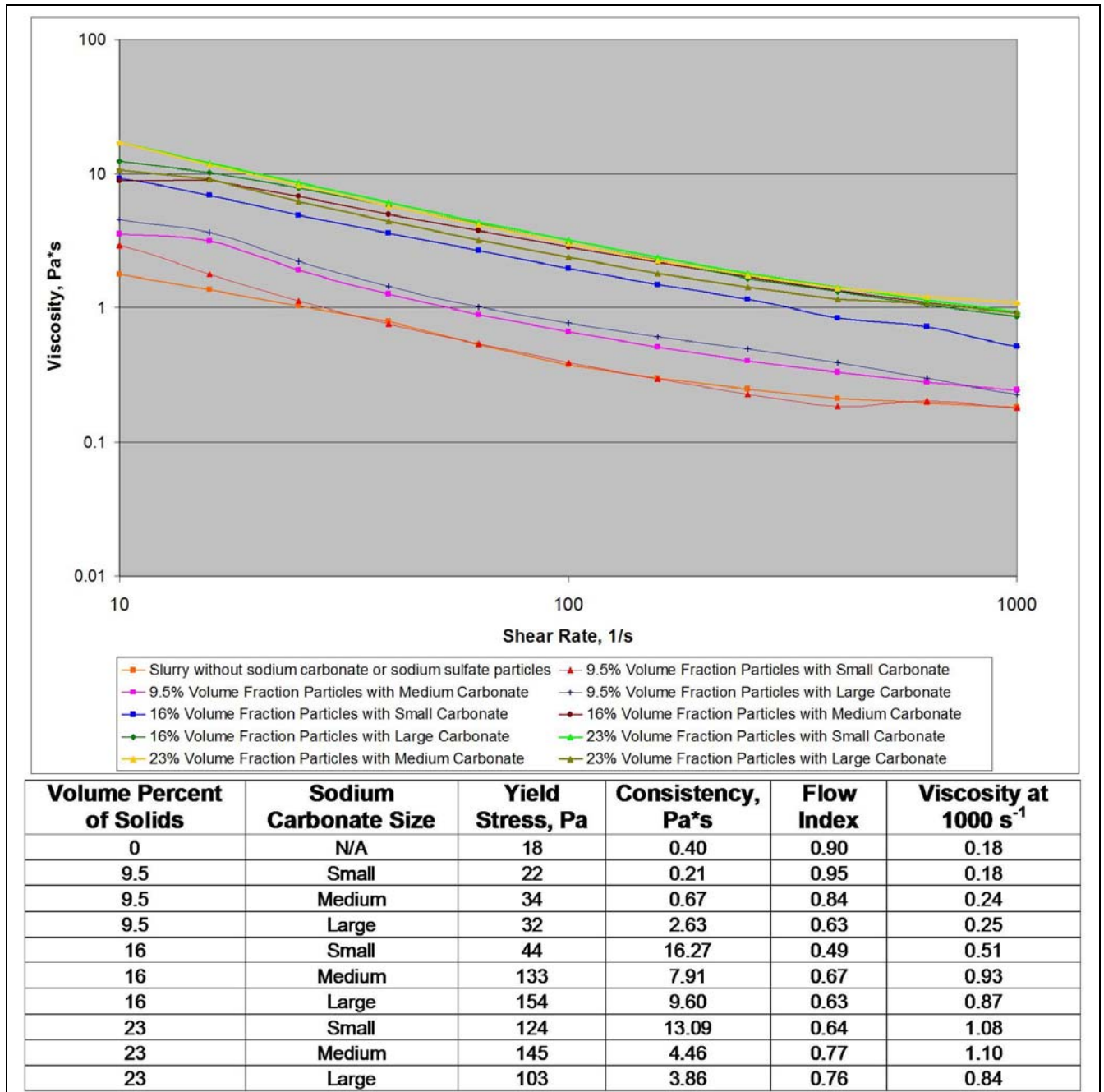
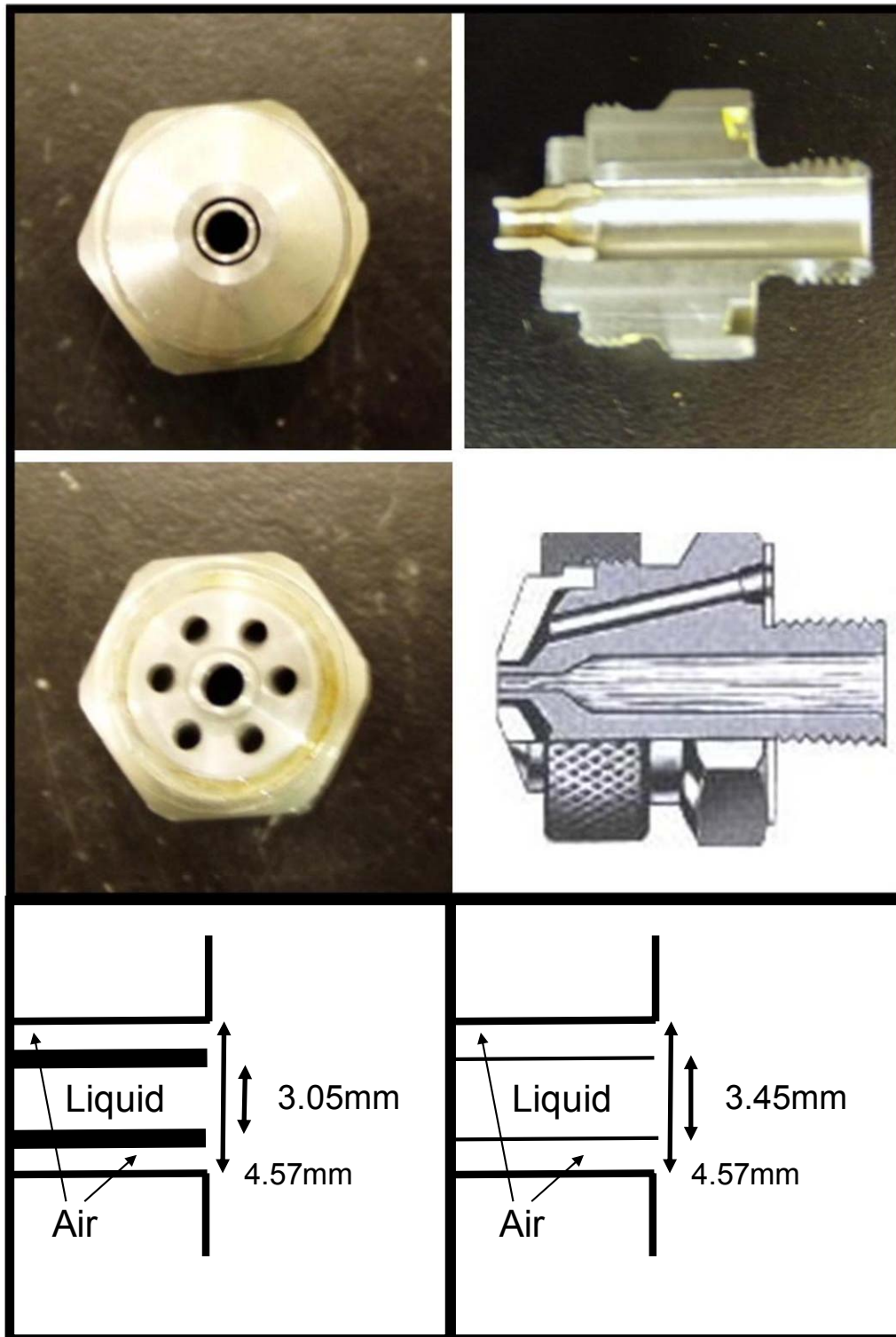
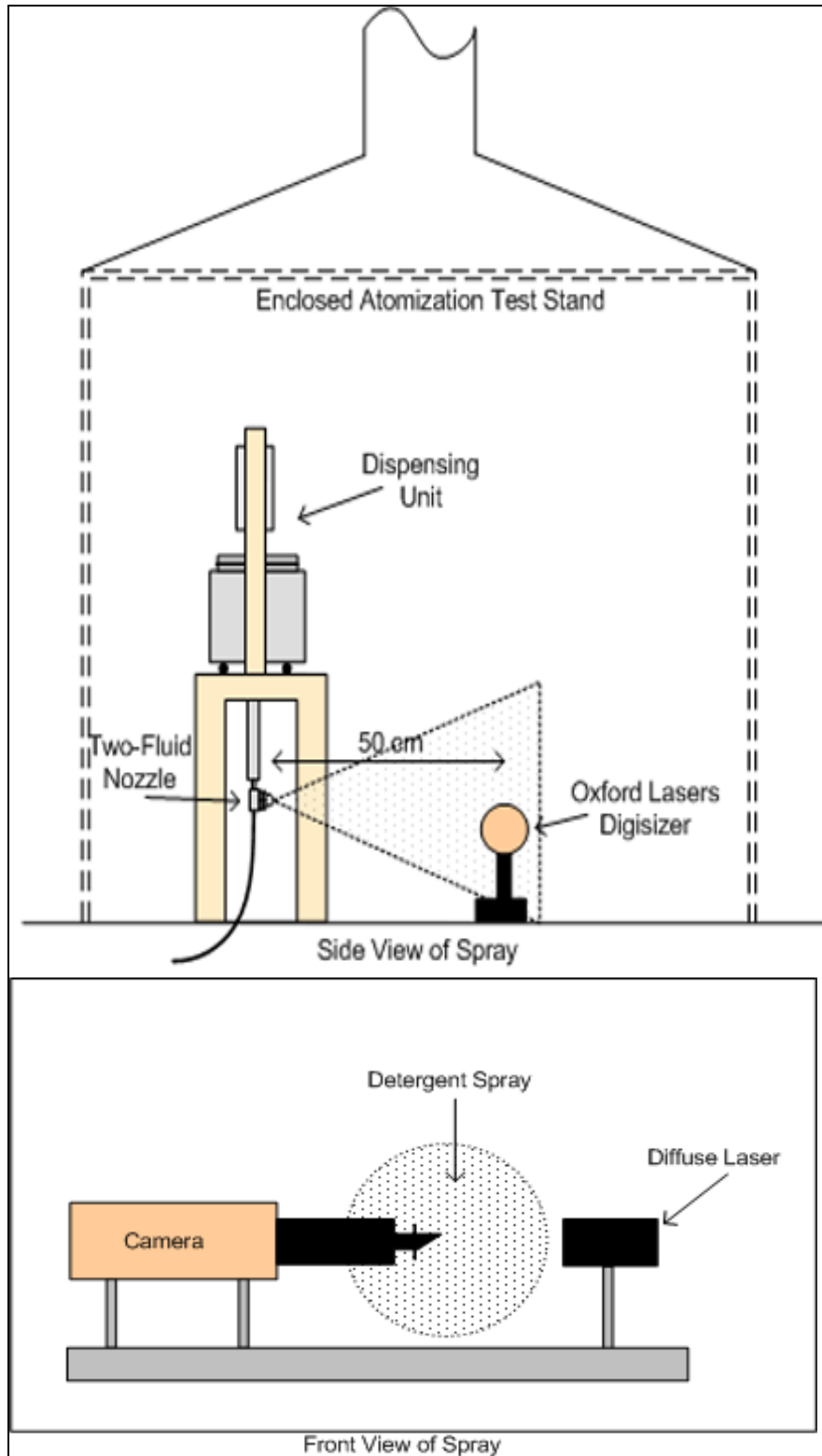


Figure 4. Slurry rheology data, Herschel-Bulkley parameters and the experimentally measured viscosity at a shear rate of 1000s<sup>-1</sup>.



**Figure 5.** Photos and diagrams of the nozzle type used. Upper right: nozzle with air cap. Liquid flow out of center opening and air flows out of annular space. Upper left: nozzle that has been cross sectioned to show internal features. Only the liquid flow path is visible. Middle left: nozzle without air cap. The six holes are for air flow that converge and exit underneath the air cap as shown on the upper left frame. Middle right: cross sectional diagram showing one of the six air channels and the liquid flow path. Lower frames: cross-section diagrams of nozzles used in this study (not to scale). Left: as-received Spraying-Systems nozzle. Right: same nozzle model drilled to a larger liquid diameter.



**Figure 6.** Experimental Apparatus.

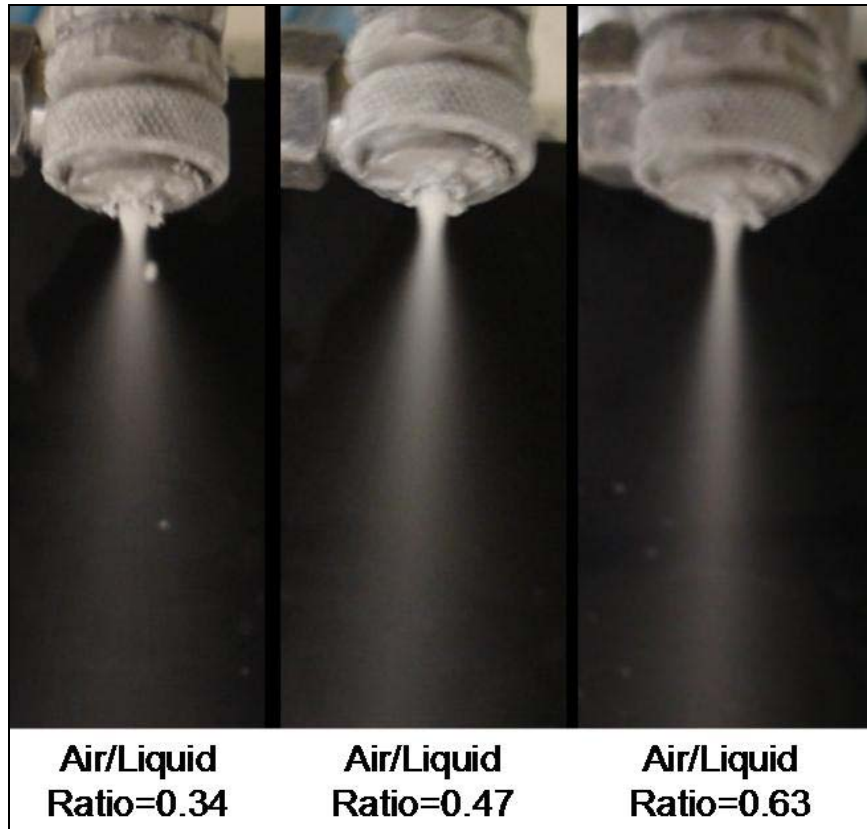


**Figure 7.** Photographs of the spray. The spray angle is clearly larger for the lower air/liquid mass ratio.

Solids Volume Percent	Sodium Carbonate Size	Nozzle Diameter, mm	Air/Liquid Ratio	$D_{v,0.1}$	$D_{v,0.5}$	$D_{v,0.9}$	Relative Span
9.5%	Small	3.05	0.34	29.5	75.0	179.7	2.00
9.5%	Small	3.05	0.47	22.4	57.2	158.3	2.38
9.5%	Small	3.05	0.63	20.8	48.9	95.1	1.52
9.5%	Small	3.45	0.34	32.1	84.9	178.2	1.72
9.5%	Small	3.45	0.47	28.5	73.1	185.0	2.14
9.5%	Small	3.45	0.63	28.5	72.8	162.1	1.84
9.5%	Medium	3.05	0.34	28.5	72.6	157.5	1.78
9.5%	Medium	3.05	0.47	22.6	59.4	139.4	1.97
9.5%	Medium	3.05	0.63	23.0	59.4	116.7	1.58
9.5%	Medium	3.45	0.34	35.4	81.1	231.6	2.42
9.5%	Medium	3.45	0.47	29.6	75.2	175.0	1.93
9.5%	Medium	3.45	0.63	27.3	66.6	161.6	2.02
9.5%	Large	3.05	0.34	30.8	74.7	140.1	1.46
9.5%	Large	3.05	0.47	22.9	59.6	136.5	1.91
9.5%	Large	3.05	0.63	24.1	67.1	213.8	2.83
9.5%	Large	3.45	0.34	29.9	65.2	137.1	1.64
9.5%	Large	3.45	0.47	25.2	59.2	120.1	1.60
9.5%	Large	3.45	0.63	25.0	57.0	113.4	1.55
16%	Small	3.05	0.34	27.7	61.0	115.4	1.44
16%	Small	3.05	0.47	25.6	59.8	129.4	1.74
16%	Small	3.05	0.63	25.2	61.5	167.8	2.32
16%	Small	3.45	0.34	27.1	71.2	141.9	1.61
16%	Small	3.45	0.47	24.7	69.0	146.7	1.77
16%	Small	3.45	0.63	23.5	68.2	134.5	1.63
16%	Medium	3.05	0.34	23.9	57.3	115.2	1.59
16%	Medium	3.05	0.47	21.5	53.4	114.1	1.73
16%	Medium	3.05	0.63	21.9	58.4	167.2	2.49
16%	Medium	3.45	0.34	26.3	61.4	135.8	1.78
16%	Medium	3.45	0.47	21.6	47.2	98.8	1.64
16%	Medium	3.45	0.63	20.1	42.1	119.0	2.35
16%	Large	3.05	0.34	26.1	62.2	146.1	1.93
16%	Large	3.05	0.47	23.9	57.9	129.7	1.83
16%	Large	3.05	0.63	24.5	64.9	196.3	2.65
16%	Large	3.45	0.34	25.7	61.4	116.0	1.47
16%	Large	3.45	0.47	23.2	55.7	139.2	2.08
16%	Large	3.45	0.63	21.7	54.0	139.0	2.17
23%	Small	3.05	0.34	24.4	59.7	105.6	1.36
23%	Small	3.05	0.47	22.2	55.2	99.9	1.41
23%	Small	3.05	0.63	22.4	56.5	121.2	1.75
23%	Small	3.45	0.34	25.2	62.1	114.1	1.43
23%	Small	3.45	0.47	23.2	57.1	110.1	1.52
23%	Small	3.45	0.63	23.1	57.7	121.9	1.71
23%	Medium	3.05	0.34	24.1	63.5	152.8	2.03
23%	Medium	3.05	0.47	21.2	54.6	124.0	1.88
23%	Medium	3.05	0.63	20.9	53.0	112.9	1.74
23%	Medium	3.45	0.34	23.9	60.1	121.6	1.63
23%	Medium	3.45	0.47	21.3	53.1	120.0	1.86
23%	Medium	3.45	0.63	21.4	55.9	172.8	2.71
23%	Large	3.05	0.34	24.3	58.8	211.9	3.19
23%	Large	3.05	0.47	20.9	50.1	132.1	2.22
23%	Large	3.05	0.63	21.2	54.4	189.3	3.09
23%	Large	3.45	0.34	23.8	60.0	156.9	2.22
23%	Large	3.45	0.47	21.1	53.2	150.2	2.43
23%	Large	3.45	0.63	21.0	53.1	282.1	4.92

**Table 2.** Data summary table for all atomization tests. The statistics  $D_{v,0.1}$ ,  $D_{v,0.5}$ , and  $D_{v,0.9}$  are the diameters that represent a volume fraction of smaller drops. For example  $D_{v,0.5}$  is the “volume median diameter”. Half the sprayed liquid volume is in drops larger than this diameter and half is in smaller drops.

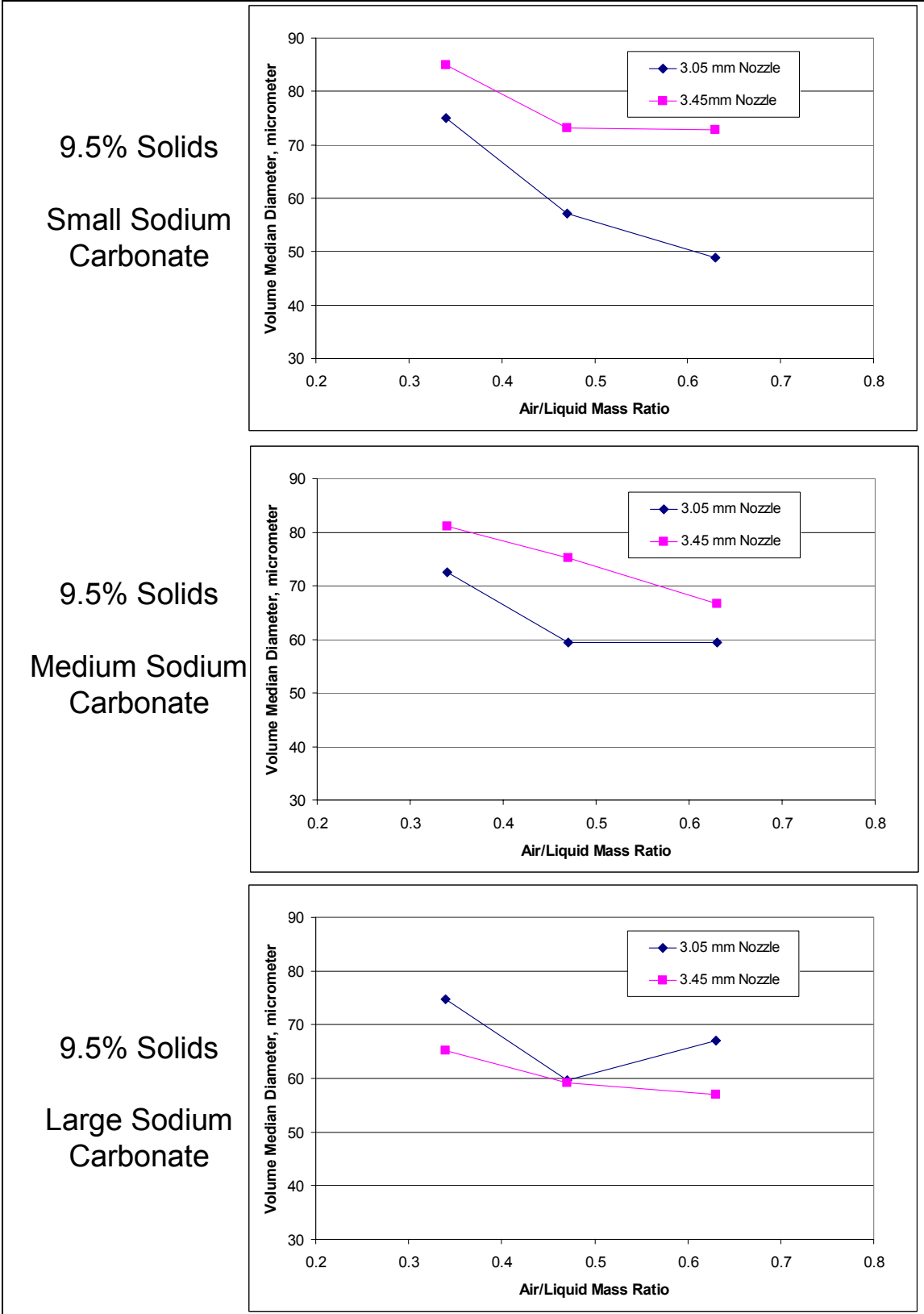


Figure 8. Volume Median Diameter ( $D_{v,0.5}$ ) as affected by air/liquid ratio and nozzle diameter for slurries containing 9.5 volume % added solids.

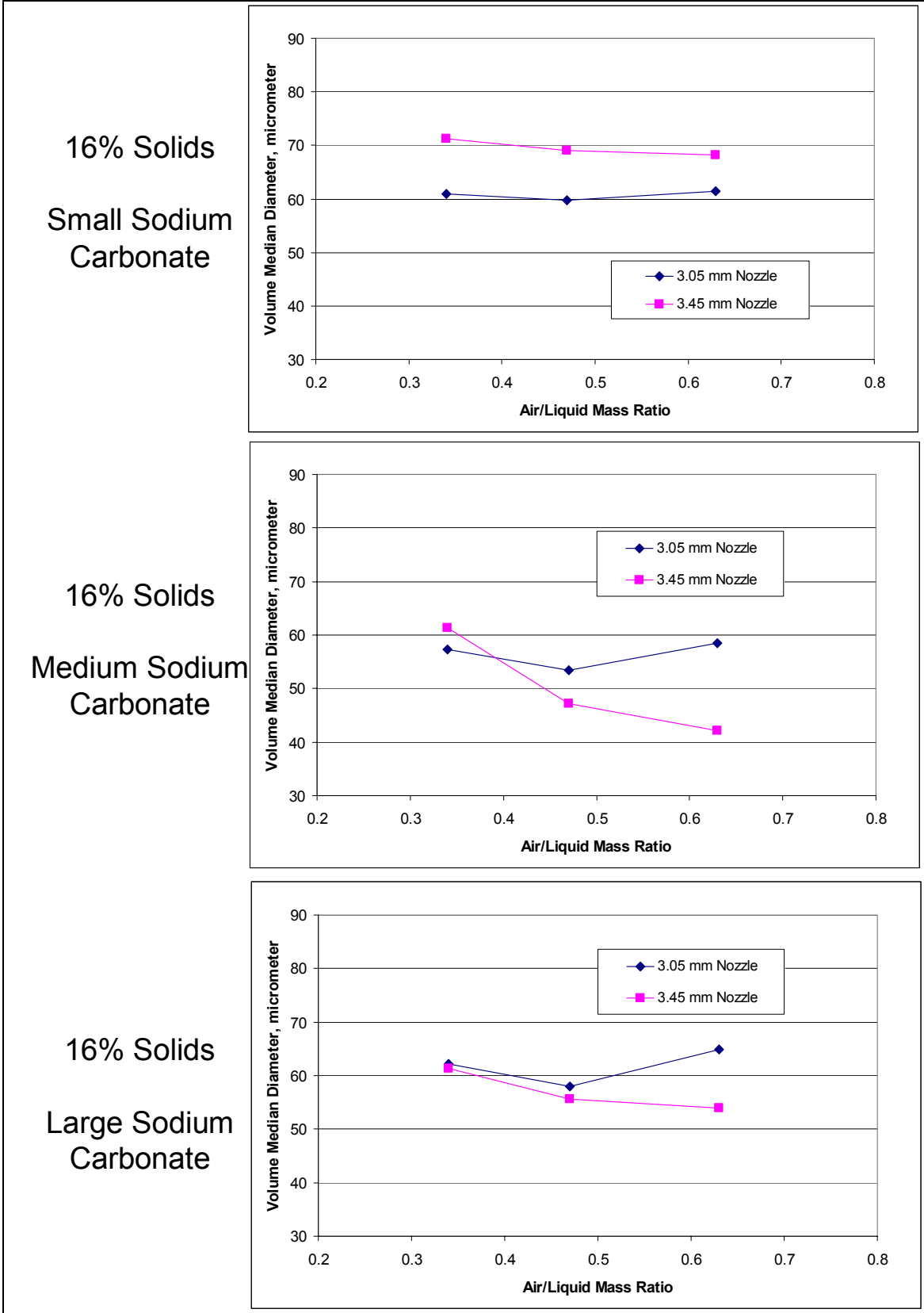


Figure 9. Volume Median Diameter ( $D_{v,0.5}$ ) as affected by air/liquid ratio and nozzle diameter for slurries containing 16 Volume % added solids.

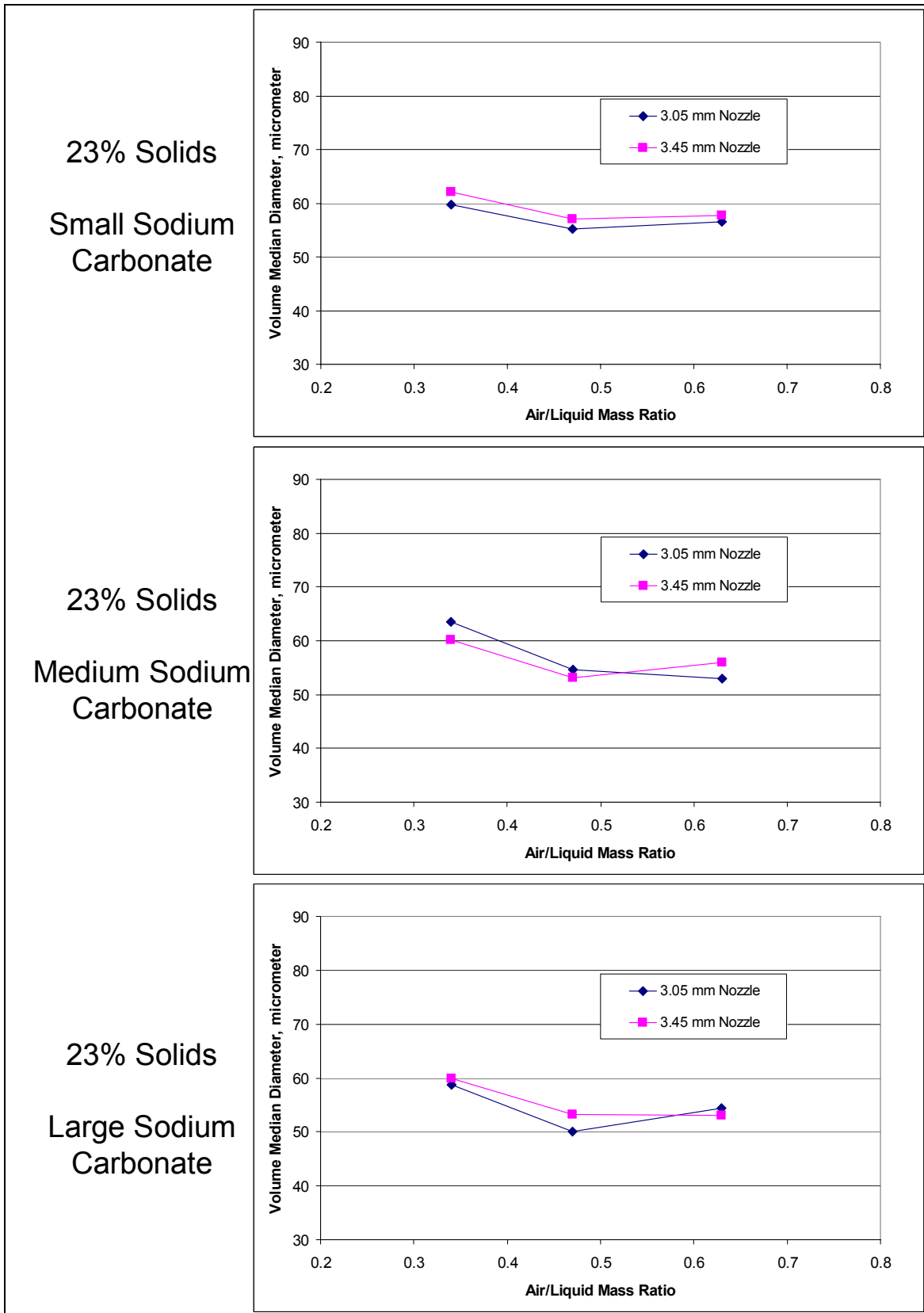
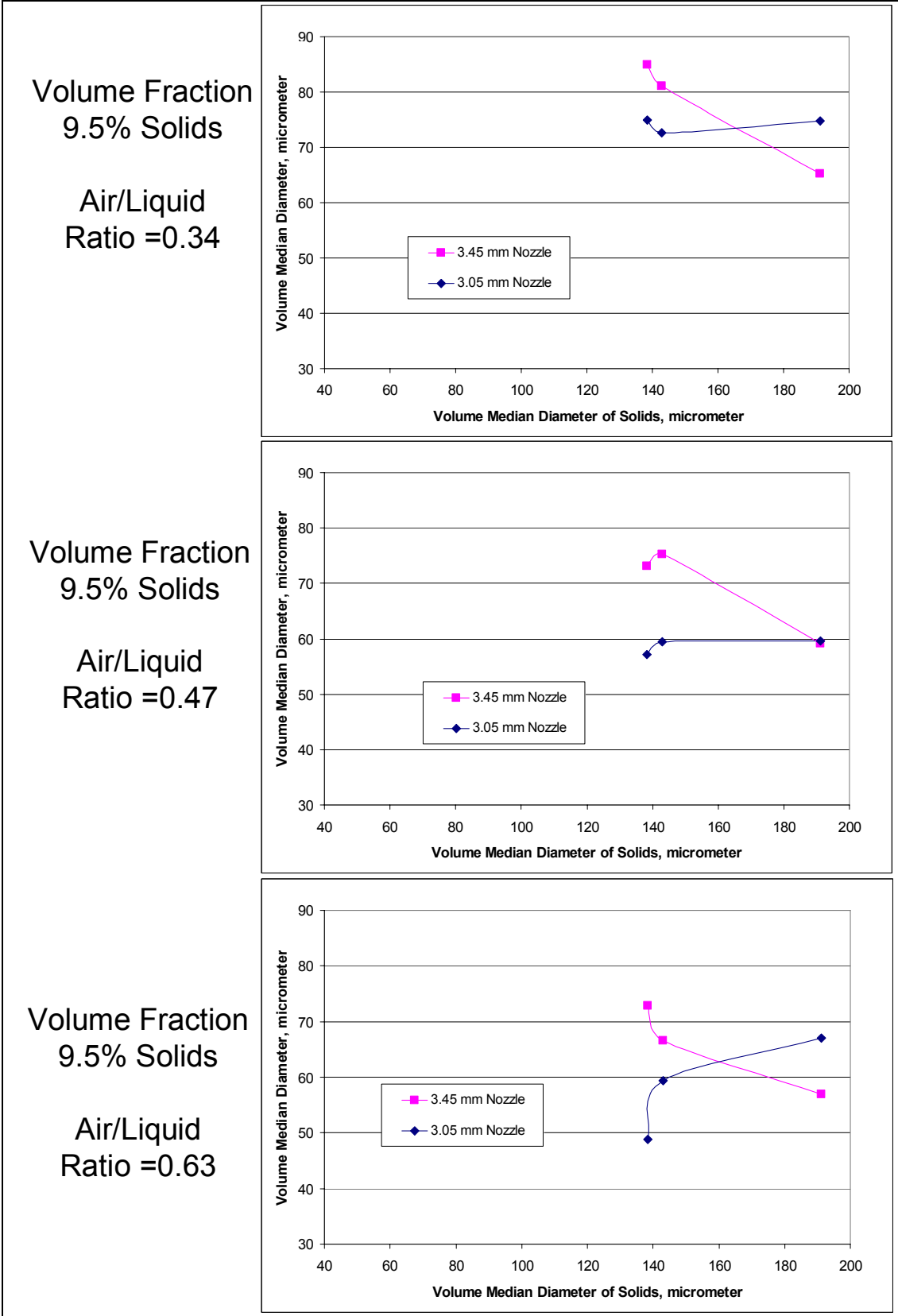
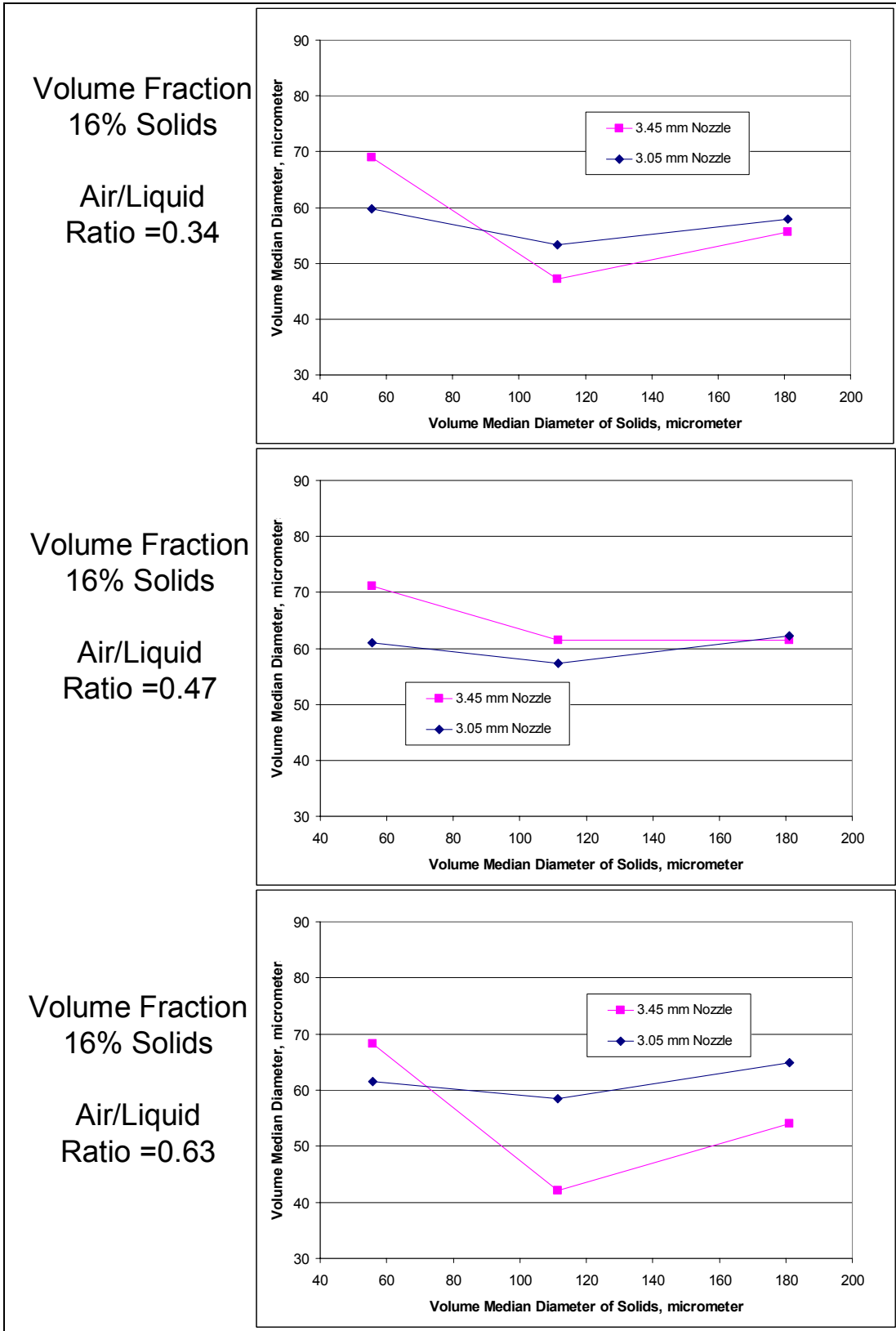


Figure 10. Volume Median Diameter ( $D_{v,0.5}$ ) as affected by air/liquid ratio and nozzle diameter for slurries containing 23 Volume % added solids.



**Figure 11.** Volume Median Diameter ( $D_{v,0.5}$ ) as affected by volume median diameter of added solids for slurries containing 9.5 volume percent added solids.



**Figure 12.** Volume Median Diameter ( $D_{v,0.5}$ ) as affected by volume median diameter of added solids for slurries containing 16 volume percent added solids.

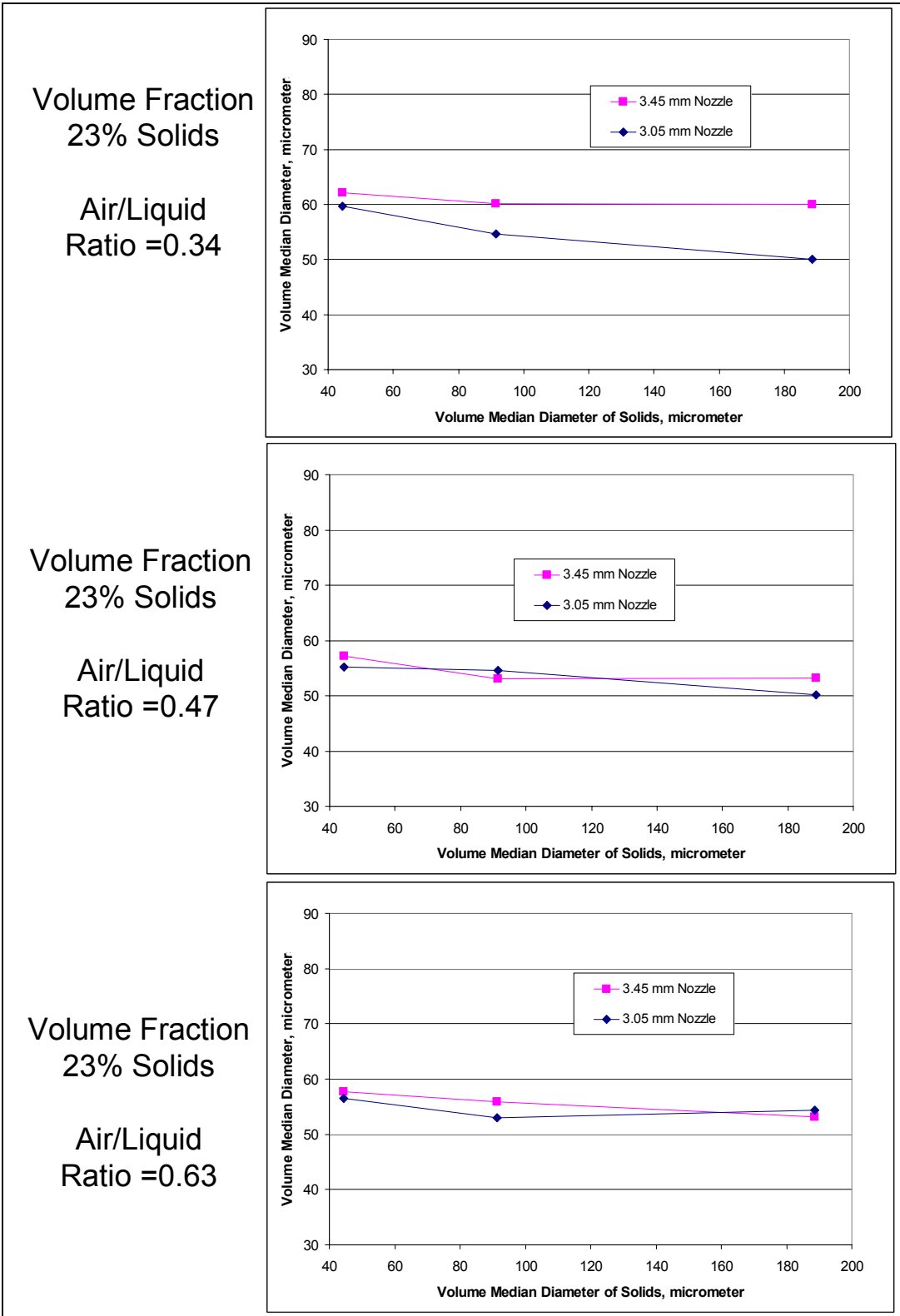
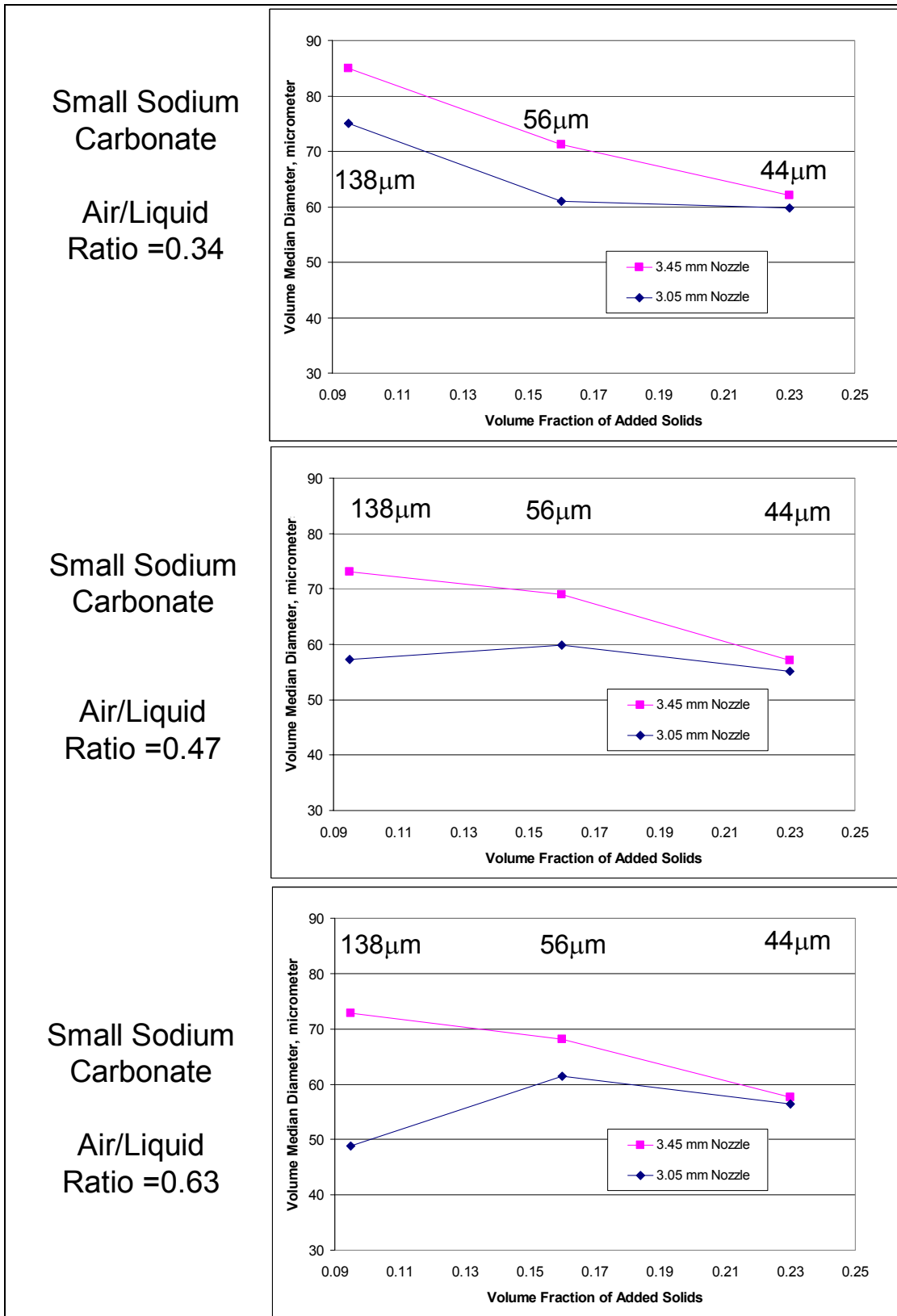
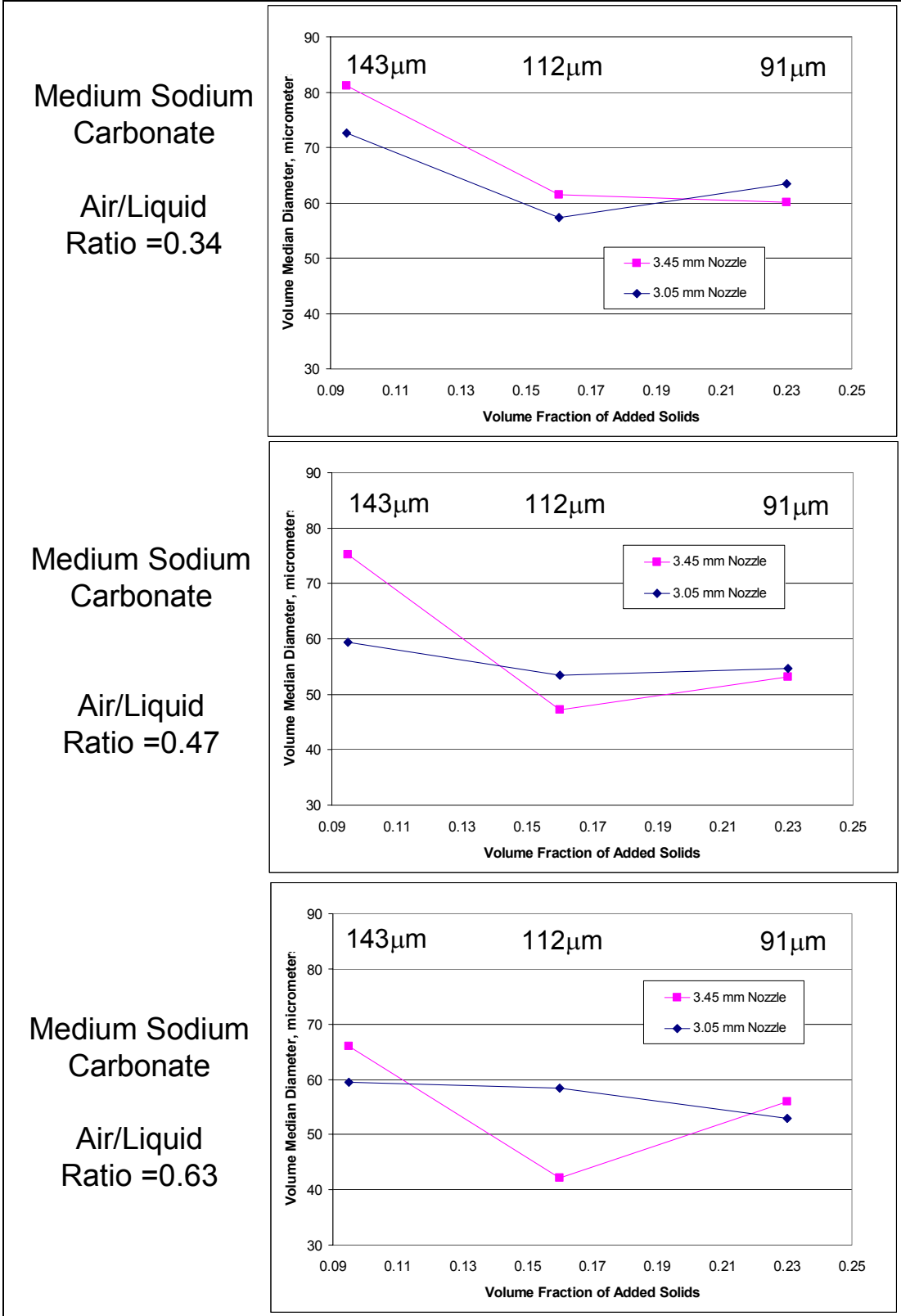


Figure 13. Volume Median Diameter ( $D_{v,0.5}$ ) as affected by volume median diameter of added solids for slurries containing 23 volume percent added solids.



**Figure 14.** Volume Median Diameter ( $D_{v,0.5}$ ) as affected by volume percent added solids for slurries containing “small” sodium carbonate particles (see Figure 1 for size data). The inset numbers refer to the volume median diameter ( $D_{v,0.5}$ ) of the added particle mixtures (sodium sulfate + sodium carbonate).



**Figure 15.** Volume Median Diameter ( $D_{v,0.5}$ ) as affected by volume percent added solids for slurries containing “medium” sodium carbonate particles (see Figure 1 for size data). The inset numbers refer to the volume median diameter ( $D_{v,0.5}$ ) of the added particle mixtures (sodium sulfate + sodium carbonate).

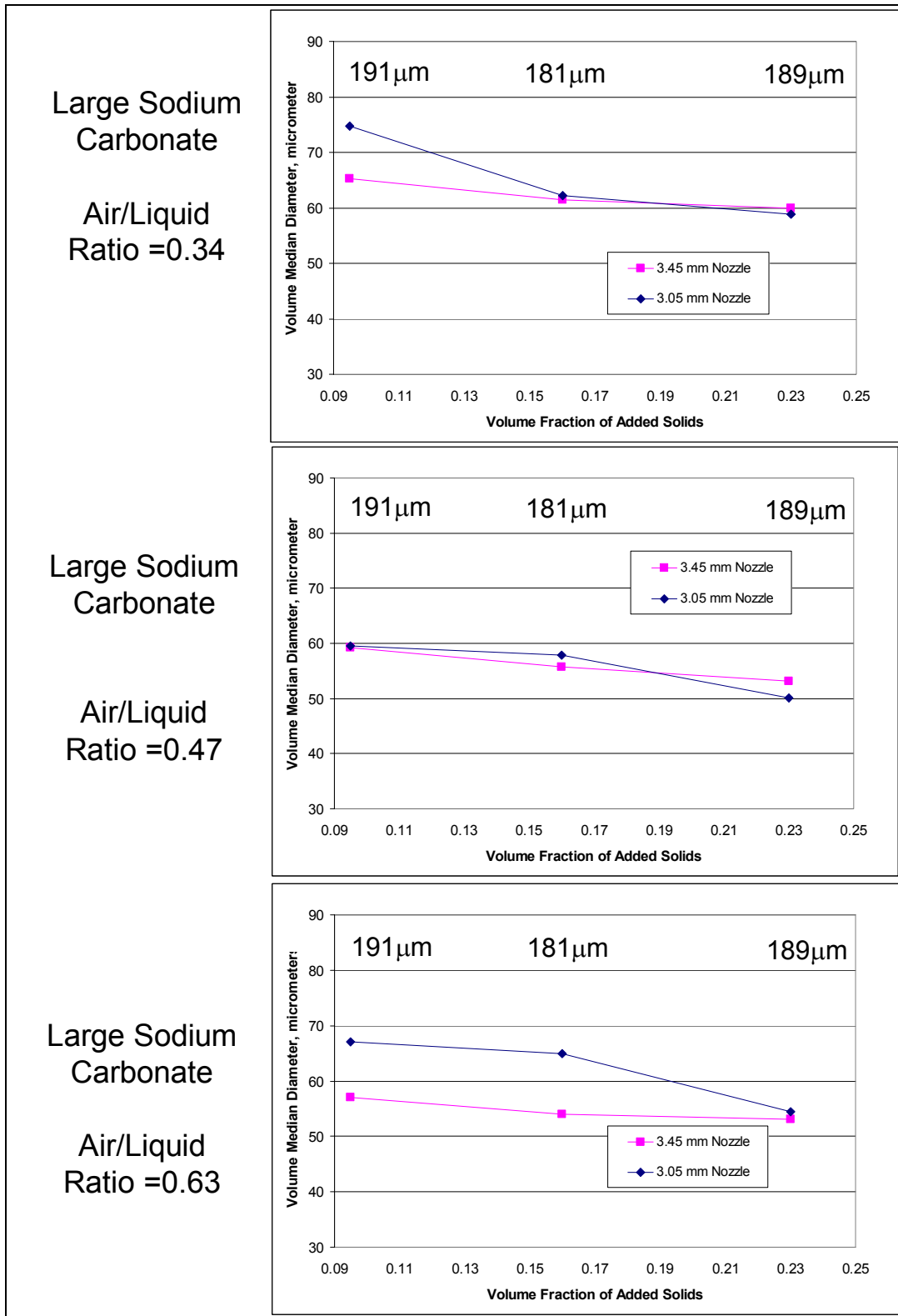


**Figure 16.** Volume Median Diameter ( $D_{v,0.5}$ ) as affected by volume percent added solids for slurries containing “large” sodium carbonate particles (see Figure 1 for size data). The inset numbers refer to the volume median diameter ( $D_{v,0.5}$ ) of the added particle mixtures (sodium sulfate + sodium carbonate).

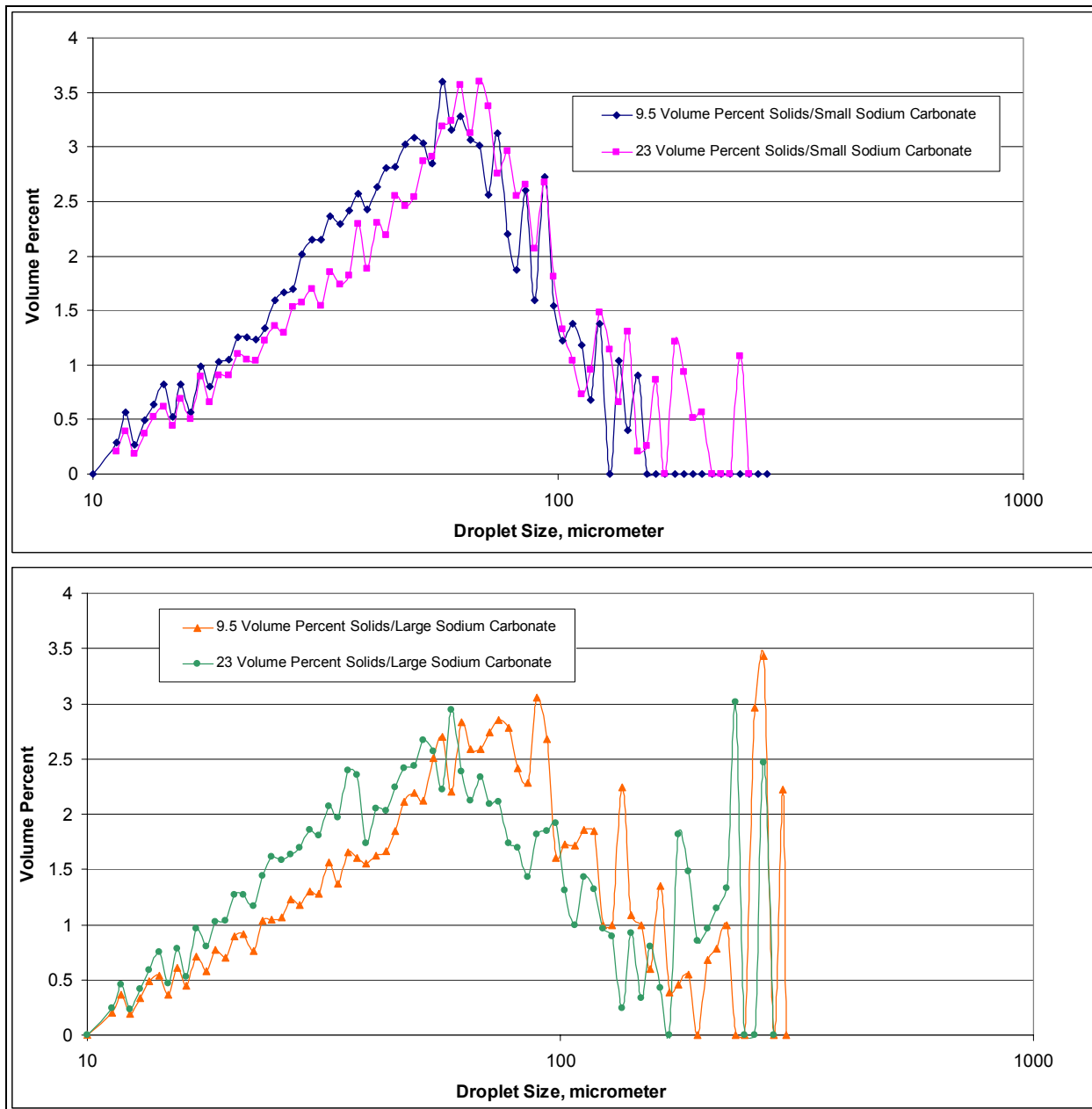


**Figure 17.** Droplet size distribution data for the 3.05 mm nozzle for the lowest (top) and highest (bottom) solids volume fractions, each with the smallest and largest sodium carbonate particles. The appearance of the distributions are “jagged” due to the high-speed photography technique. This technique literally counts the droplet and assigns them to size bins without smoothing the raw data or fitting to a model.